Proposed evaluation method for three-point bending beam tests of fiber reinforced concrete

Dr. Péter Károly Juhász[1]

[1] : JKP STATIC Ltd., Budapest, Hungary.

Abstract

Fiber reinforced concrete (FRC) is a composite material whose post-crack response is highly dependent on the properties of the mixed fibers, as well as their position and orientation in the matrix and on the fracture surface. To determine the material parameters of fiber reinforced concrete, a relatively small, notched beam with a cross-section of 125 × 150 mm is used in the European test standard. Although a uniform distribution is assumed, this is not the case in the small beam test. The coefficient of variation of the residual test results is usually high, which can be attributed to the relatively small size of the specimen and the random location of the fibers. This large scatter of the results leads to a low characteristic value during the traditional statistical evaluation, which results in an uneconomic design. Furthermore, the fibers were aligned to the longitudinal axis of the beam during production, which also led to an unrepresentative value.

When evaluating material parameters, ignoring the number, distribution, and location of fibers intersecting the fracture cross-section can lead to uneconomical, ineffectual, or even exaggerated material parameters. It is therefore necessary to modify and supplement the actual test standards.

In this paper, a mixing model is presented to determine the number of fibers intersecting the cross-section at a certain fiber geometry and dosage. The effect of mixing is demonstrated using measures of fiber-moment and uniformity. Different methods for the determination of the fiber-moment are presented, and the accuracy and sensitivity of these methods are also investigated. The values obtained are compared with the results of laboratory tests on steel and synthetic FRC. At the end of the experiment, the correlation between fiber-moment and residual strength is presented, along with the correlation coefficients.

A novel extended test method for the evaluation of beam test results using these methods is presented. The method allows more accurate mean, characteristic, and design material parameters to be determined.

Keywords

Fiber reinforced concrete, three-point bending test, evaluation of beam test results, mixing model

1 Introduction

Fiber reinforced concrete (FRC) is a composite material wherein the matrix is composed of concrete (Kollár 2003). Fibers can be made of different materials (steel, plastic, glass, and natural) and have different geometries (diameter, length, and shape) (ACI, 2009). The mixed fibers increase the fracture energy of concrete and thus its ductility (Gopalaratnam et al., 1991; Balaguru, Shah, 1992). When significant residual strength is required after concrete cracking, the most widely used fibers in the industry are steel and synthetic macrofibers.

Using fiber reinforcement reduces the cracking sensitivity of concrete and increases its service life. It is used primarily in industrial floors and shotcrete but also in precast concrete in many applications, although no design standard is available. Design methods can be found in guidelines, such as the *fib* Model Code 2010 (2012). There are several standards for establishing the material parameters for design, the most common of which are the bending beam and center-loaded panel tests. Among beam tests, three- and four-point bending tests are widely used, and European standards use the three-point notched beam test (EN 14651:2005+A1:2007). The force, deflection, and crack mouth opening displacement (CMOD) are measured.

The dispersion of the three-point notched beam test results was large because of the small reference area (125 × 150 mm) and random location of the fibers. Owing to the large scatter, the characteristic values of the material parameters were significantly reduced, leading to an uneconomical design and use. Using mathematical statistics, it has been shown that, assuming a random distribution, variance decreases as the reference area increases (Juhász, 2018). Bernard increased the size of circular panels and experimentally demonstrated a significant decrease in variance (Bernard, 2013). However, testing larger test specimens under standard laboratory conditions is challenging and less widespread. A more favorable evaluation could be obtained using a more suitable probability distribution function (Bernard and Xu, 2007) or by extracting the intrinsic variability by simulating the probabilistic distribution and mechanical response of each fiber (Cavalaro, Aguado, 2015). The effect of the large scattering due to the small reference cross-section is considered by the *fib* Model Code 2010 (2012) by employing a factor to increase the residual stress value for structures with sufficiently large cross-sections. A new method for determining the characteristic values was presented by Juhász (2020), which was based on the relationship between the residual stress values of the beams and the real distribution of fibers in the broken cross-section.

The location of the fibers in the fracture cross-section was random but assumed to be uniform. The dispersion of the number of fibers can be estimated by analytical mixing models; however, their location in the fracture cross-section significantly influences the efficiency of the fibers in beam-bending tests. Barros (2005) investigated the relationship between the number of fibers passing through the cross-section and the residual stress value but did not consider the location of the fibers. The number of fibers passing through the cross-section was determined by Dupont and Vandewalle (2005), who considered the formwork effect. Despite the significant importance of fiber spacing in the cross-section, research focusing on it has been scarce.

This study investigated the locations of steel and synthetic fibers on the cross-section and their effects on the residual strength. A mixing model was devised to estimate the number of fibers intersecting the cross-section. The model was used to investigate the number of fibers and their locations, and the results were compared with experimental results.

2 Modelling the number and position of fibers intersecting a cross-section using a mixing model

The number of fibers intersecting the cross-section was determined by Naaman (1972) using geometric probability. Consider a fiber with its center in volume *V* and investigate its intersection with crack plane *A* (Figure 1a). If the center of the fiber is less than $0.5l_f$ from the crack plane, the fiber may intersect depending on its orientation (Figure 1b).

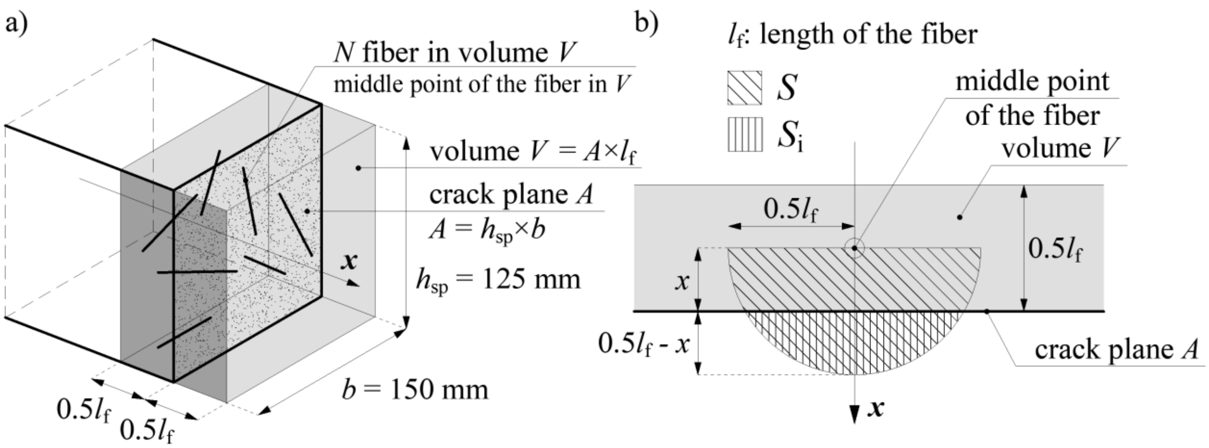

Figure 1: a) Crack plane A and volume V; b) geometric probability of intersection

This probability is the ratio of the surface area of the spherical cap S_i to that of S (Figure 1b).

$$q_{\mathrm{Naaman}} = \frac{S_{\mathrm{i}}}{S} = \frac{0{,}5l_{\mathrm{f}} - x}{0{,}5l_{\mathrm{f}}} = 1 - \frac{2x}{l_{\mathrm{f}}} \tag{1}$$

The probability of intersection of a single fiber in volume *V* is:

$$p = \frac{\int_0^{l_f/2} \left(1 - \frac{2x}{l_f}\right) dx}{l_f/2} = 0.5 \tag{2}$$

The derivation holds for an infinite cross-section; however, for a finite cross-section, the orientation of the fibers is affected by the formwork around the cross-section, which is called the wall effect in literature. This has been investigated by Dupont and Vandewalle (2005) and Stroven (2010) for steel fibers and by Alberti et al. (2017) and Juhász (2018) for steel and synthetic fibers. For steel and synthetic fibers, the degree of the formwork effect is negligible for standard beam cross-sections; therefore, it is not necessary to consider it when determining the number of fibers passing through the cross-section (Juhász, 2018).

The probability of the intersection of a single fiber in volume *V* is 0.5. According to the central limit theorem, a random variable with a binomial distribution can be approximated well by a normal distribution under certain conditions, provided that (Ekstrom and Rensen, 2014):

$$N \times \min \begin{Bmatrix} p \\ 1-p \end{Bmatrix} \geq 5 \rightarrow N \geq 10 \tag{3}$$

If the number of fibers with the middle point in volume V is $N \geq 10$, the intersection is well approximated by a normal distribution. The mean values of the number of fibers intersecting the cross-section and dispersion are:

$$m = N_{\mathrm{m}} = Np = 0.5N \tag{4}$$

$$\sigma = \sqrt{Np(1-p)} = \sqrt{0.25N} \tag{5}$$

The moment resistance of a cracked FRC section depends on the number and z-directional location of the fibers intersecting the fracture cross-section. If the force in the fibers is assumed to be uniform, the moment of the fibers farther away from the compressed edge would be greater than the fiber closer to the compressed edge (Figure 2). The lever arm of the fibers was measured from the top edge of the beam, neglecting the thickness of the compressed zone and summing them. The resulting value is the *fiber-moment* of the fibers (Juhász, 2018):

$$S_{\mathrm{f,test,e}} = \sum_{i=1}^{N_{\mathrm{d}}} z_{\mathrm{i}} \tag{6}$$

where S_{f} is the fiber-moment in meters, z_{i} is the z-directional distance from the compressed edge for fiber i, and N_{d} is the number of fibers intersecting the cross-section (Figure 2).

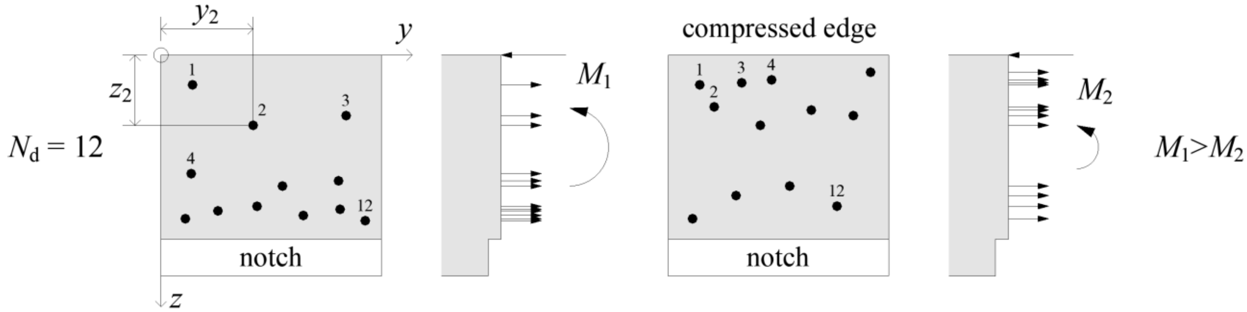

Figure 2: Effect of intersecting fibers on the moment resistance of the cracked cross-section

The exact measurement is a time-consuming method; however, in the case of counting the fibers in strips, as shown in Figure 3, it is much less laborious.

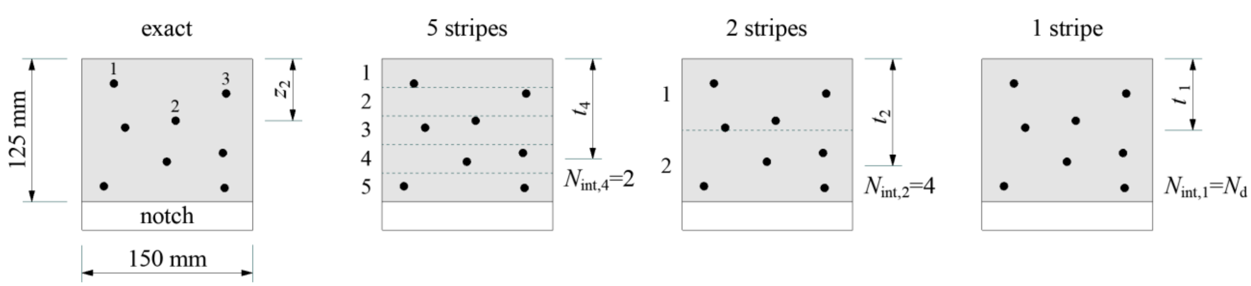

Figure 3: a) Exact method; b) 5 stripes method; c) 2 stripes method; d) 1 stripe method

This study entailed a comparison of the fiber moments determined by the exact and strip methods. The fiber moment calculated according to the strip method is as follows:

$$S_{\mathrm{f,test,s}} = \sum_{i=1}^{s} N_{\mathrm{int,i}} t_{\mathrm{i}} \tag{7}$$

where s is the number of strips, $N_{\mathrm{int,i}}$ is the number of fibers in strip i, and t_{i} is the distance between the middle point of the strip i and the compressed edge.

Assuming uniform mixing and orientation, the number of fibers intersecting the cross-section is N_{m} according to Equation (4). Assuming that the distribution of the fibers in the cross-section is uniform, the center of the intersecting fibers coincides with the center of the fracture cross-section, so that the fiber-moment can be written as:

$$S_{\mathrm{f,ideal}} = N_{\mathrm{m}} 62.5\,\mathrm{mm} \tag{8}$$

The Clark–Evans aggregation index (nearest neighbor analysis) was used to characterize the uniform distribution of fibers in the cross-section:

$$R = \frac{r_{\mathrm{A}}}{r_{\mathrm{E}}} = \frac{2\sqrt{N_{\mathrm{d}}/A}\sum_{i=1}^{N_{\mathrm{d}}} r_{\mathrm{i}}}{N_{\mathrm{d}}} \tag{9}$$

where r_{i} is the distance to the nearest neighbor fiber of fiber i, R is the aggregation index, A is the fracture surface according to Figure 1. R is close to 0 when fibers are clustered and close to 1 when fibers are randomly spaced. R equals 2.149 for fibers that are spaced in a triangular lattice arrangement, i.e. perfectly regular.

3 Laboratory testing of FRC beams

3.1 Test method and specimens

The test was performed according to EN 14651:2005+A1:2007 standard. The beam was notched at a depth of 25 mm on one side at the center of the beam, and the crack opening was measured at this notch (Figure 4a). The size of the fracture cross-section was 125 × 150 mm. The test was a three-point bending test with supports at 500 mm. The test was CMOD-controlled, where the CMOD rate was 0.05 mm/min up to CMOD = 0.1 mm and then 0.2 mm/min. The result was the force–CMOD diagram (Figure 4b).

FRC beams made with steel and synthetic macrofibers were tested with dosages corresponding to the usual dosage in the industry: 20 and 30 kg/m^3 for steel fibers and 2.5, 5.0, and 7.5 kg/m^3 for synthetic fibers. The geometrical properties of the fibers are shown in Table 1. The concrete mix design was based on the reference concrete specification EN 14845-1:2008, whereas the aggregate grading was according to EN 1766:2017. During the experiment, the beams were prepared and stored in accordance with EN 12390-2:2019.

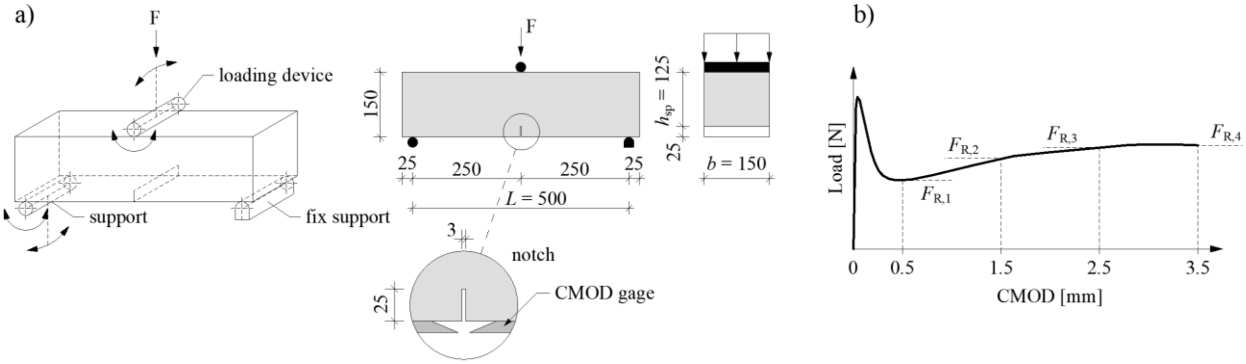

Figure 4: a) Three-point bending beam test (EN 14651:2005); b) Typical Load–CMOD diagram

Table 1: Fiber geometry

Property	Steel fiber	Synthetic fiber
Diameter/length (l_f), mm	1/50	0.7/48
Fibers/kg	3 177	54 545
N in V at 1 kg/m^3 dosage (assuming perfect mixing)	2.919	49.090

3.2 Evaluation of results

The residual stress was evaluated at specific CMOD values (CMOD = 0.5, 1.5, 2.5, and 3.5 mm) according to EN 14651:2005+A1:2007. The residual strength of each specimen was determined according to Equation (4) of EN 14651:2005+A1:2007.

After the test, the beams were broken into two parts, and the location of the fibers on the beam cross-section was measured to the nearest 0.1 mm according to the coordinate system shown in Figure 2. In the case of steel fibers, the fibers are typically pulled out; conversely, in the case of synthetic fibers, some fibers are pulled out and some ruptured. The identification of pulled-out fibers was more accurate; conversely, in the case of fibers that ruptured in the concrete, only one side of the fiber was visible, which could lead to inaccuracies during counting. Furthermore, synthetic fibers are often positioned close to each other, making measurement difficult.

Our measurements aimed to determine the fiber moments. In the calculation, the pulled-out fibers are included at full value; however, for the ruptured fibers, it must be considered that they appear in both cross-sections; that is, they were calculated at half the value of the number of fiber determinations.

4 Comparison of the mixing model and laboratory results

4.1 Number of fibers intersecting the cross-section

The mean value of fibers intersecting the cross-section (N_d) was determined after the beam tests. Likewise, the analytical value of the mixing model (N_m) was also determined. The results are compared and shown in Figure 5.

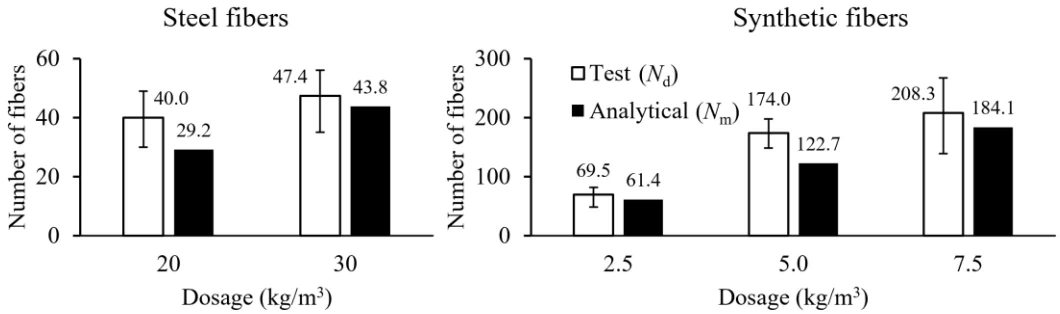

Figure 5: Mean and range of the number of fibers intersecting the tested cross-sections (N_d), the mean value of the mixing model for steel and synthetic fibers (N_m)

The coefficients of variation (CV) of the test (cv_t) and model ($cv_m = \sigma/m$) were determined and are presented in Table 2. The comparison shows that the number of fibers intersecting the cross-section determined from the mixing model was always smaller than the values from the tests. This is because of a modification in the orientation of the fibers during vibration, which is along the longitudinal axis of the beam. The relative dispersion of the mixing results decreased with increasing fiber number; however, this contrasted with the experimental results. The value of the relative dispersion of the model was significantly different from the experimental results. Nevertheless, the sample size of this study was small.

Table 2: Coefficients of variation of the test and model

Fiber type and dosage	**Number of fiber *N* in volume *V***	**CV of the test, cv_t [%]**	**CV of the model, cv_m [%]**
Steel – 20 kg/m^3	58.388	14.5	13.1
Steel – 30 kg/m^3	87.583	14.2	10.7
Synthetic – 2.5 kg/m^3	122.726	18.5	9.0
Synthetic – 5.0 kg/m^3	245.452	12.2	6.4
Synthetic – 7.5 kg/m^3	368.178	23.8	5.2

4.2 Uniformity of fibers and its relationship with fiber-moment

The uniform distribution of fibers across the cross-section is well characterized by the Clark–Evans aggregation index *R*, which is determined for each cross-section using Equation (8) (Figure 6).

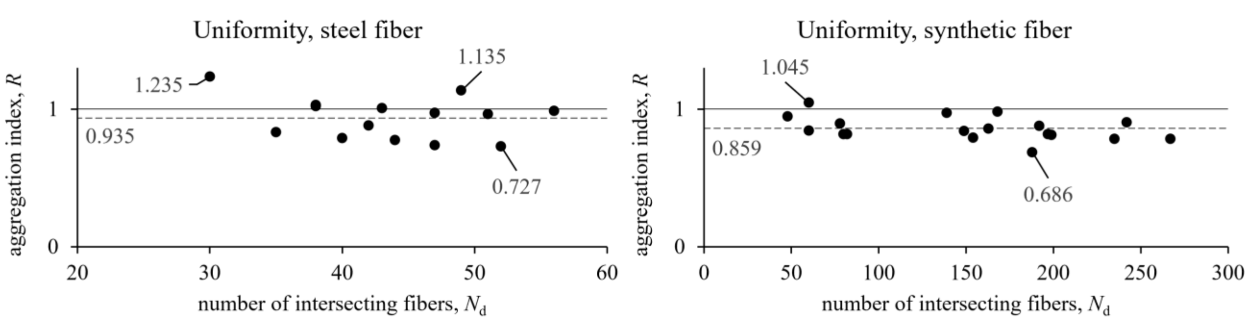

Figure 6: Distribution of fibers as a function of the number of fibers intersecting the cross-section for steel and synthetic fibers

The fiber-moment calculated from one strip assumed an ideal distribution because the lever arm was measured from the middle point of the cross-section (Figure 3d). Based on this, the fiber-moment of one strip is a function of the fiber number (N_d), as indicated by the dashed line in Figure 7. Generally, the fiber moment of 1 strip includes no information regarding the location of the fibers and assumes a perfect distribution. The deviation of the exact fiber moment from this value provides important information regarding the location of the fibers.

In Figure 8, the correlation between the deviation of the exact fiber-moment from the ideal fiber-moment and uniformity is plotted. It can be seen that there are cross-sections where the fiber moment is close to the ideal fiber moment and the uniformity is good (steel: 20 kg/m^3–7 and synthetic: 2.5 kg/m^3–5) or where the fiber moment deviates significantly from the ideal but has a good uniformity (synthetic: 2.5 kg/m^3–6). In some cross-sections, fiber moment deviation and uniformity are poor (steel: 30 kg/m^3–7).

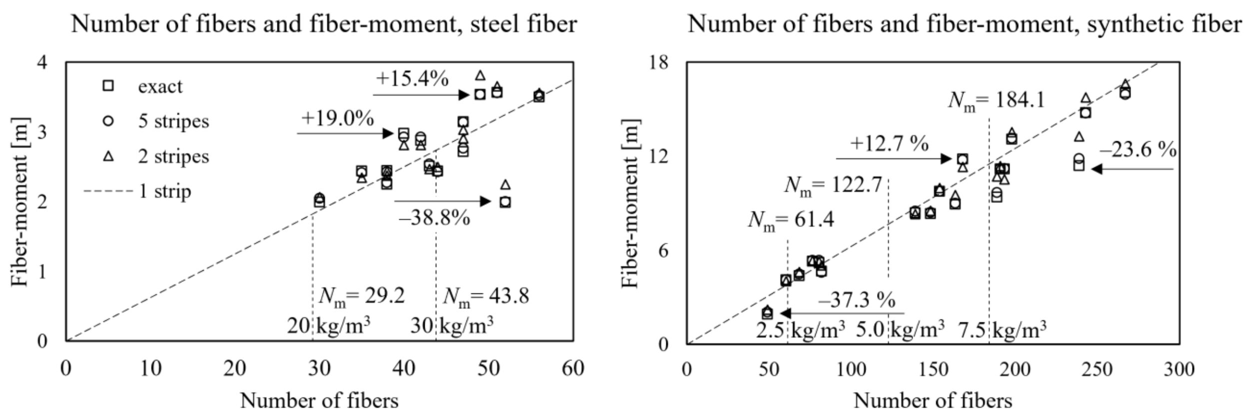

Figure 7: Number of fibers and fiber-moment correlation

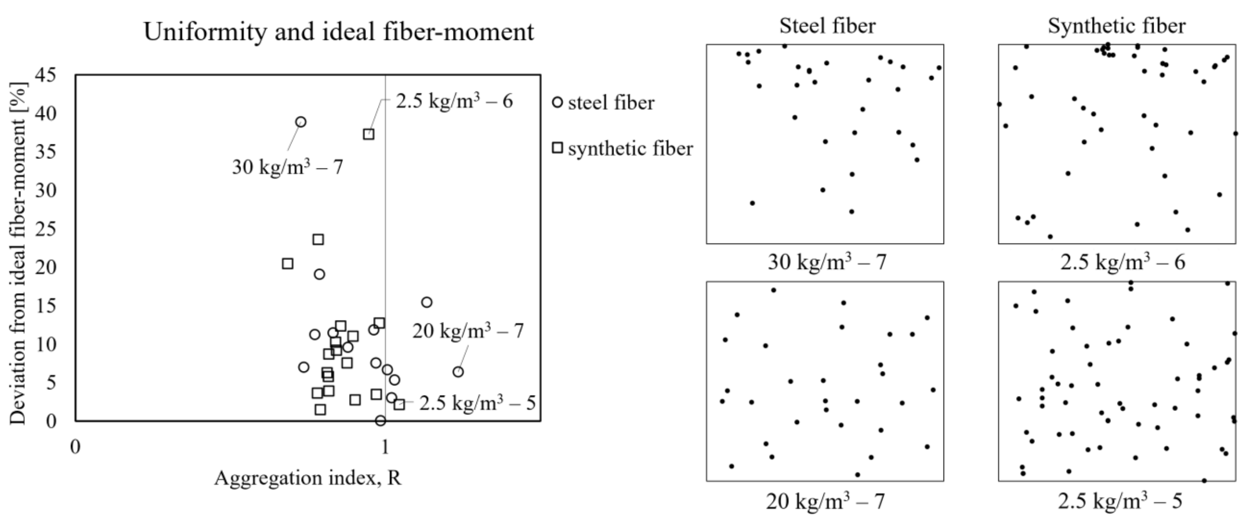

Figure 8: Correlation of uniformity and deviation from the ideal fiber-moment with the beam sections of extreme cases

4.3 Relationship between residual stresses and fiber-moments

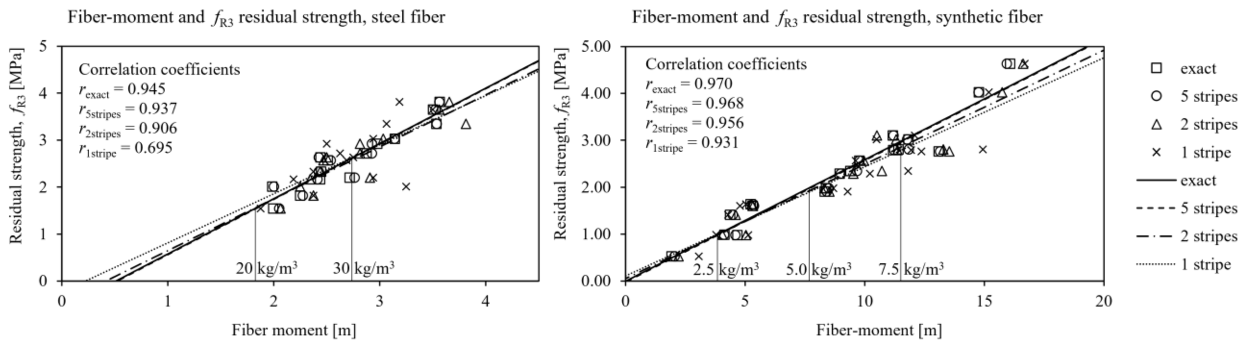

Figure 9: Relationship between the fiber-moment and residual strength f_{R3} in the case of steel and synthetic fibers

As per the correlation coefficients, the exact and 5-band methods give a reliable value. The ideal fiber-moments for different dosages are indicated.

5 New direction for the evaluation of FRC beam testing

The standard beam tests were used to determine the material parameters of FRC materials. The tests show that the variation of the results was very large, which confirms the similar results obtained in the literature and laboratories. For the determination of design material parameters, the referenced standards (ISO 2394, EN 1990:2011), assuming a normal distribution, use a statistical method to determine the characteristic value (5% lower quantile) as follows:

$$f_{R,i,k} = f_{R,i,m}\left(1 - k_n V_x\right) = f_{R,i,m} - k_n s_x \tag{10}$$

where $f_{r,i,k}$ and $f_{R,i,m}$ are the characteristic and mean values of residual stresses, respectively, V_x= $s_x/f_{R,i,m}$ is the coefficient of variation, s_x is the standard sample deviation, and k_n is a factor dependent on the number of specimens according to EN 1990:2011. The standard distinguishes between *known* and *unknown* coefficient of variation, V_x. Unknown is when the V_x is determined on the basis of the specimens tested. Known is when the V_x has been determined from a large number of previous test data. For known V_x, the k_n values give a more favorable result. In case of synthetic fiber used in this research a good estimation is $V_{x,known}$=25% if the dosage if above 5 kg/m^3.

The characteristic values were highly dependent on the number of samples and the variance of the results. In certain cases, a $k_n s_x$ member can cause the characteristic value to be negative (Juhász, 2020), which is useless. However, in several cases, the large scatter in the results is because of the uneven distribution of fibers on the fracture surface of some beams, which causes the fiber-moment to increase or decrease significantly. Ignoring the fiber-moment results in significantly lower values during the evaluation and determination of the characteristic results. The mixed fibers in the beam were oriented toward longitudinal axis of the beam during vibration, which results in more fibers intersecting the cross-section than in the case of a larger specimen. Using the mixing model and the ideal fiber-moment derived from it, the positive and negative effects can be eliminated, and a material parameter closer to reality can be determined for engineering purposes. The exact method for determining the characteristic values was detailed by Juhász (2020).

6 Concluding remarks

The use of fiber reinforced concrete in the industry is growing because of the design methods recommended in the guidelines. It is primarily used in industrial floors and tunnels; moreover, it is increasingly used in roads and railway slabs as primary reinforcement and as additional reinforcement in reinforced concrete structures. To determine the material parameters of the fiber reinforced concrete, a three-point beam-bending test was performed, as specified in EN 14651:2005+A1:2007. In the evaluations, the scatter of the results was large, even with the highest attention, because of the location of the fibers within the cross-section, which is a characteristic of fiber reinforced concrete. In the present study, the location of fibers on the fracture cross-section, the uniformity of their distribution, and their effect on the fiber moment were investigated. The results indicate a strong correlation between the fiber-moment and the residual strength, and by investigating and considering this correlation in the evaluation, more accurate and economical material parameters that are closer to reality can be determined. The original standardized test procedure does not need to be changed when applying this method; only an additional study is undertaken. The number of fibers is determined via visual inspection, which has an inherent error that cannot be ignored. However, in my previous research, the application of this method proved to be sufficiently accurate.

7 References

ACI Comittee 544 (2009), *Report on Fiber Reinforced Concrete (Reapproved 2009)*, ACI 544.1R-96, American Concrete Institute, ACI Farmington Hills.

Alberti, M.G., Enfedaque A. and Gálvez, J.C. (2017), *On the prediction of the orientation factor and fibre distribution of steel and macro-synthetic fibres for fibre-reinforced concrete*, Cement and Concrete Composites 77, pp. 29–48.

Balaguru, P.N. and Shah, S.P. (1992), *Fiber-Reinforced Cement Composites*, McGraw-Hill, New York.

Barros, J.A.O., Cunha, V.M.C.F., Ribeiro, A.F. and Antunes, J.A.B. (2005), *Post-cracking behaviour of steel fibre reinforced concrete*, Materials and Structures 38, pp. 47–56.

Bernard, E.S. (2013), *Development of a 1200-mm-Diameter Round Panel Test for Post-Crack Assessment of Fiber-Reinforced Concrete,* Advances in Civil Engineering Materials 2, no. 1, pp. 457–471.

Bernard, E.S. and Xu, G.G. (2007), *Statistical Distribution of Fiber-Reinforced Concrete Beam Test Data*, Journal of ASTM International 4, no. 3, pp. 1–12.

Cavalaro, S.H.P. and Aguado, A. (2015), *Intrinsic Scatter of FRC: An Alternative Philosophy to Estimate Characteristic Values*, Materials and Structures 48, no. 11, pp. 3537–3555.

Dupont, D. and Vandewalle, L. (2005), *Distribution of steel fibres in rectangular sections*, Cement & Concrete Composites 27, pp. 391–398.

Ekstrom, C.T. and Sørensen, H. (2014), *Introduction to Statistical Data Analysis for the Life Sciences*, Chapman and Hall/CRC, New York.

fib, International Federation for Structural Concrete (2012), *Model Code 2010*, Final Draft, Volume 1, fib Bulletin no. 65, International Federation for Structural Concrete, Lausanne, Switzerland.

Gopalaratnam, V.S., Shah, S.P., Batson, G., Criswell, M., Ramakishnan, V. and Wecharatana, M. (1991), *Fracture Toughness of Fiber Reinforced Concrete*, ACI Materials Journal 88, no. 4, pp. 339–353.

Juhász K.P. (2018), *The effect of synthetic fibre reinforcement on the fracture energy of the concrete*, Doctoral dissertation, Budapest University of Technology and Economics.

Juhász K. P. (2020), *A proposed evaluation method for three-point beam tests of fiber-reinforced concrete*, ASTM Journal of Testing and Evaluation, Volume 49, Issue 5.

Kollár L.P. and Springer, G.S. (2003), *Mechanics of Composite Structures*, Cambridge University Press, Cambridge, UK.

Naaman, A.E. (1972), *A statistical theory of strength for fiber reinforced concrete*, Doctoral thesis, Massachusetts Institute of Technology.

Stroven, P. (2010), *Methodology of modelling fiber reinforcement in concrete elements*, in B.H. Oh et al., (editors) Fracture mechanics of concrete structures – high performance, fiber reinforced concrete, special loadings and structural applications. Korea Concrete Institute, Seoul, pp. 1418–1424.